The Crystal Computer:
Computing with Inorganic Cellular Frameworks and Nets

Mark D. Symes, University of Glasgow, UK

Leroy Cronin, University of Glasgow, UK

ABSTRACT

The enormous potential of parallel computing has led to the first prototype devices being constructed. However, all the examples to date rely on complicated chemical and/or physical manipulations, and hence do not lend themselves to the kind of widespread investigation necessary to advance the field. This article presents a new paradigm for parallel computing: the use of solid, single crystalline materials as cellular automata suggesting the idea of the "Crystal Computer," now possible due to a new class of crystalline cellular materials that undergo single-crystal-to-single-crystal (SC-SC) oxidation and reduction (REDOX) reactions. Two avenues are proposed for investigation: reversible single-crystal to single-crystal electronic transformations and solid-state spin transfer within spin-crossover complexes. Both schemes allow computation to occur in three dimensions, within cheap and easy to assemble materials and using commonplace techniques for input and readout.

Keywords: *Cellular Automata, Crystal Computer, Parallel Computing, Polyoxometalate, Spin Cross-Over*

INTRODUCTION

Cellular Automata (CAs) as postulated by von Neumann (von Neumann, 1951) and Conway (Gardner, 1970) constitute an area of intense study on account of their potential for parallel computing (de Silva & Uchiyama, 2007; Credi, 2008; Jones, 2009). The most basic form of such automata is a grid of squares (or "cells") which may be colored either black or white and which are capable of changing their color in response to the colors of their neighboring cells according to defined laws. By varying these laws and the initial distribution of black and white cells (the input to the system), patterns can be created out of apparent disorder by repeatedly applying the over-riding laws to each successive "generation" of cells. These patterns can be viewed as the output of a computational sequence by the cellular array, and it has been shown that CAs of this type are Universal Turing Machines (Turing, 1937; Berlekamp *et al.,* 2003) capable of computing anything that can be computed algorithmically.

Recent practical examples of functioning CA based on chemical systems include automata capable of modeling cancer cell proliferation (Bandyopadhyay *et al.*, 2010) and playing simple "games" against a human opponent (Pei *et al.*, 2010). However, these surface-confined

DOI: 10.4018/jnmc.2011010103

Figure 1. Photograph of crystals of $\mathbf{1}_{ox}$ *with schematic showing how triangular (green) and tetrahedral (red) units link up in three dimensions to produce an infinite 3,4-connected framework*

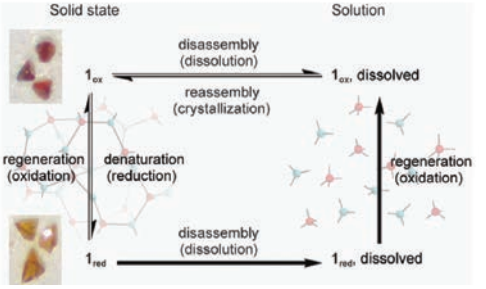

systems are yet to exploit the inherently three dimensional nature of chemical interactions fully and as a consequence the computing power of such 2-D devices may be limited by these geometrical constraints. Specifically, creating *real-world* CA capable of acting as true Universal Turing Machines remains an enormous challenge. These extant real-world systems also rely on time and labor-intensive techniques for data input and read-out, such as scanning-tunnel microscopy (Bandyopadhyay *et al.*, 2010) and/or "wet chemical" manipulations (Pei *et al.*, 2010).

Herein, we propose an approach to cellular automata based on single crystal-single crystal (SC-SC) transformations driven by optical and/or electrical impulses supplied to the crystal by simple and readily available equipment. Two possible systems will be expounded, both with the potential for three-dimensional computing using very simple apparatus under standard "bench-top" conditions (e.g. room temperature and pressure). The first relates to work performed in the Cronin group on reversible electron uptake and loss leading to SC-SC transformations in crystals of composition $[(C_4H_{10}NO)_{40}(W_{72}M_{12}O_{268}Si_7)]\cdot 48H_2O$ ($M = Mn^{III}$ or Co^{III}) (Ritchie *et al.,* 2008; Thiel *et al.,* 2009; Thiel *et al.,* 2010). The second approach relies on the phenomenon of spin cross-over within certain crystalline materials (Gütlich *et al.,* 2000; Turner & Schultz, 2001; Halcrow, 2008; Bodenthin *et al.*, 2009).

CRYSTAL COMPUTING WITH POLYOXOMETALATES

Crystals of the form $[(C_4H_{10}NO)_{40}(W_{72}M_{12}O_{268}Si_7)]\cdot 48H_2O$ ($M = Mn^{III}$) ($\mathbf{1}_{ox}$) self-assemble from a solution of the well-studied tungsten polyoxometalate $[\gamma\text{-}SiW_{10}O_{36}]^{8-}$ and a simple manganese(II) salt and hence are straightforward to prepare. The structure of these crystals comprises an infinite array of 3- and 4-connected Keggin polyanions (Long *et al.,* 2010), where each three connected unit is surrounded by three neighboring clusters in a trigonal-planar fashion, and each 4-connected unit features four nearest neighbors located on the vertices of a distorted tetrahedron (Figure 1).

The linkages between the clusters in Figure 1 are [W-O-Mn] bridges, which can be considered as "bolts" holding together the tetravacant $\{SiW_8O_{36}\}$ (tetrahedral) and trivacant $\{SiW_9O_{37}\}$ (trigonal-planar) building blocks. These bridges have no preferred orientation, and so statistically half of the linkages are between an Mn on a tetravacant cluster and a W on a trivacant cluster and the other half are between a W on a tetravacant cluster and an Mn on a trigonal cluster. We can thus begin to generate some simplified schemes representing the molecular structure within these crystals which will demonstrate their potential as CA grids (Figure 2).

Figure 2a shows a 2-D slice through a crystal of form $\mathbf{1}_{ox}$, with tetrahedral cross-sec-

Figure 2. (a) Schematic representation of a two-dimensional slice through the infinite 3,4-connected network shown in Figure 1. Red triangles show the 2-D projection of tetrahedral building blocks, blue triangles and lines show the 2-D projection of triangular building blocks in the plane and orthogonal to the plane of the paper, respectively. (b) The introduction of green circles, or nodes, shows where Mn-O-W bridges are located. Each node can "hold" one electron. (c) The most basic repeat pattern of nodes is shown by the large blue triangles. Each triangle contains 12 nodes, corresponding to the crystal unit cell $[(C_4H_{10}NO)_{40}(W_{72}M_{12}O_{268}Si_7)]\cdot 48H_2O$. (d) A representation showing just these unit cells, showing a basic CA grid.

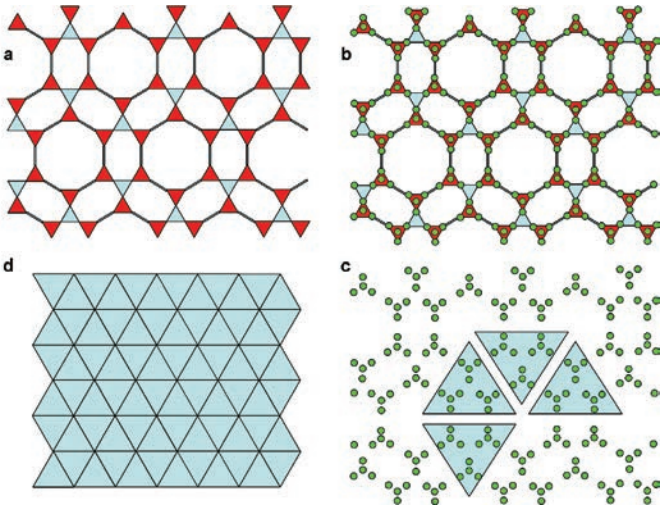

tions shown as red triangles and trigonal planar cross sections shown as blue triangles or blue lines for triangles in and orthogonal to the plane of the paper respectively. In Figure 2b, nodes (green circles) are shown corresponding to the location of [W-O-Mn] bridges between tetrahedral and trigonal units. Nodes in the center of tetrahedral units connect to vertices of trigonal units in layers above and below the plane of the paper respectively. The pattern that the nodes within a layer make is then shown in Figure 2c, which also shows how such a 2-D layer can be represented by interconnecting trigonal units (Figure 2d, *vide infra*). Note that the actual connectivity of such nets is in *three* dimensions, not just two: the 2-D representations in Figure 2 are for illustrative purposes only.

Selective chemical or electrochemical reduction (gain of electrons) of nets such as $\mathbf{1}_{ox}$ can then be achieved, corresponding to the addition of one electron to the Mn^{III} units in the [W-O-Mn] bridges to give [W-O-Mn^{II}] units (the W centers remain unchanged during this conversion). Hence by control of the reduction potential applied, a number of electrons equal to the number of Mn^{III} centers (or nodes in Figure 2b) in the net can be injected into the system, until all the Mn centers are in the Mn^{II} state. Subsequent application of an appropriate potential in the opposite direction will then convert all the Mn^{II} centers back to their original Mn^{III} state, without any degradation of the overall structure of the nets, and this is uniquely possible with these crystals due to the simultaneous proton transfer process that accompanies the electron transfer, see Scheme 1.

Crystallographically, these nets have a unit cell (the smallest repeating unit of the structure) of formula $[(C_4H_{10}NO)_{40}(W_{72}M_{12}O_{268}Si_7)]\cdot 48H_2O$, where M is a metal center capable of reversibly accepting and losing one electron. This suggests that the smallest number of electrons that can be gained or lost by the nets to yield *stable* configurations will be multiples of

Scheme 1. Chemical formulae corresponding to the SC-SC redox transformation

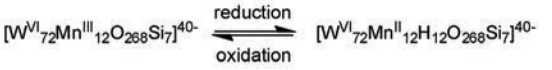

twelve. Using this structural information, inspection of Figure 2c (depicting only the nodes of the net) evinces 12-electron (12-node) "triangles" which in turn can be considered as a single cells on a simplified 2-D automaton grid (Figure 2d). Hence a fully reduced (Mn^{II}_{12}) cell would constitute a filled cell for such an automaton whilst a fully oxidized set of bridges (Mn^{III}_{12}) would act as an empty cell (Figure 3a). This forms the first putative rule of these CA. Rules 2 and 3 follow on from a combination of Rule 1 and the assumption that the system will tend to adopt the most energetically stable (lowest energy) configuration available to it. Hence Rule 2 states that a cell can only be completely filled or completely empty - there are no partially filled cells. The physical basis for this assertion is that fully reduced (Mn^{II}_{12}) cells are spatially larger than fully oxidized cells (Mn^{III}_{12}), by 3137 $Å^3$ or 5.48% (Ritchie *et al.,* 2008). Hence reduced nodes will tend to clump together so as to minimize distortions in the crystal lattice caused by the differences in size between oxidized and reduced areas. Rule 3 then expands this principle of energy minimization to how whole cells interact with each other - filled cells will tend to "stick" to each other in groups so as to minimize the collective surface area they display to the rest of the grid. Manipulation of a few simple groups of filled cells show that the surface area is lowest when the most symmetrical structures are adopted (Figure 3a). The final rule we shall consider at this stage relates to movement of cells. Figure 3b shows the proposed movement of a group of filled cells through an otherwise empty grid. Rule 4 then states that a filled cell may move to a neighboring empty cell with which it shares an edge provided that, after each filled cell from one generation has moved no more than once, the overall surface area of the filled cell ensemble in the resulting new generation is no greater than in the previous generation. This prevents automata from moving energetically uphill, in violation of the second law of thermodynamics. From this rule, we can predict that initially randomly spread groups of cells will coalesce into ever larger and more symmetrical groups through random, though constrained, "diffusion" reminiscent of Brownian Motion (Brown, 1866).

Interestingly, we find that some initial states (e.g. six adjacent filled cells in the 2-D representation shown in Figure 4a) rapidly form highly symmetrical shapes which are then prevented from further "Brownian" movements by Rule 4. Once formed, these species remain fixed until a "mobile" group of cells collides with them. Mobile groups of cells are capable of adopting two or more lowest-energy conformations between which they interconvert at random, sometimes producing a net displacement of the ensemble (Figure 4b). Collision of two ensembles then leads to a period of readjustment to a lowest-energy conformation (or potentially to just a sufficiently low local energy minimum), which could be either static or mobile. We note that the system shown in Figures 3 and 4 necessarily involves the conservation of charge (such that the number of filled cells is always conserved), in contravention of the rules for CA such as Conway's Game of Life (Gardner, 1970). However, the proposed mechanism of read-out from these systems (detection of current at the crystal face, *vide infra*) means that immobile groups of cells can be considered as computationally "dead" (in the parlance of the Game of Life), and thus the computational output of the system (current at the crystal face) need not be conserved. This offers the potential for such systems to function as close analogs to Universal Turing Machines.

To add further complexity to the system, consider the effect of applying a moderate

Figure 3. (a) Filled cells are depicted as red triangles, empty cells are shown as light blue triangles. Both shapes in Figure 3(a) consist of 10 filled cells, but the upper shape has a "surface area" of length 10, whilst the lower configuration has a surface area of length 8 and is therefore the more stable configuration. (b) The black arrows show how the movement of the cells as defined by Rule 4 permits the automaton to re-arrange to the lower energy configuration in a single generation in this example.

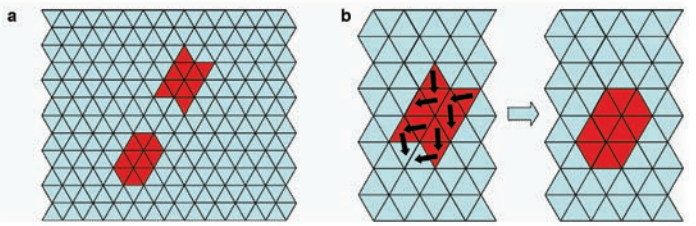

Figure 4. (a) Arbitrarily distributed cells form a highly symmetrical shape. Movement of these cells in future generations is then not allowed, as any movement would result in a higher surface area than the starting configuration. (b) A configuration of 9 cells arbitrarily re-arranges through states with the same surface area before forming a configuration (generation 3) which is capable of translation of the entire ensemble (as opposed to simply gyrating around a fixed point). Sustained movement in one direction will, however, only be maintained under the influence of a bias.

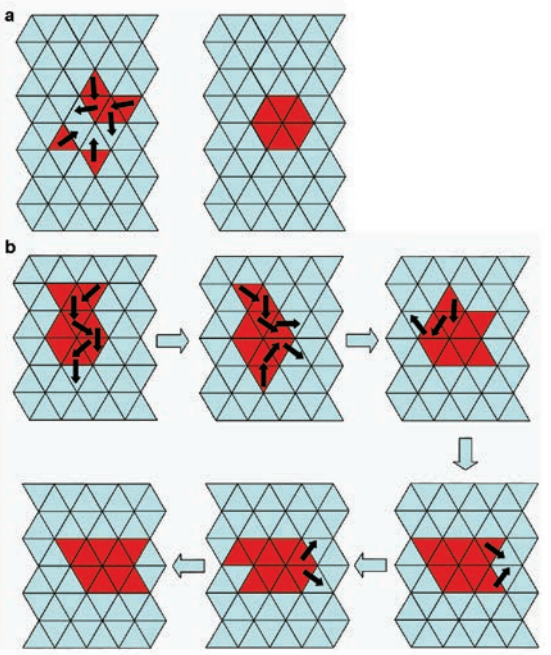

potential across the entire crystal, insufficient for additional electron injection into the material, but capable of biasing the motion of electrons (filled cells) in the lattice. Static groups of cells should remain unaffected by this bias, but mobile groups would experience a net force in a particular direction, and this would cause the evolving patterns in the lattice to slowly move in that direction. Depending on the size of the bias, and the nature of the colliding groups of cells, we can expect various patterns of filled cells not only to move through the lattice in a directed sense, but also undergo transformations specific to both their current configuration and the strength of the applied bias (and also reflecting the microscopic defects present in the array). In this sense, the initial configuration and the variable bias applied to the system can be considered as inputs and the resulting distribution of cells at a given point in time as the output at that point in time.

The way in which electrons move through the lattice shown in Figures 1 and 2 permits the interrogation of such CA using *Percolation Theory* (Broadbent & Hammersley, 1957). This theory allows predictions to be made about the time needed for a liquid applied on one face of a porous material to reach the opposite face, based upon the likelihood of two neighboring pores being connected to each other (such that the liquid can percolate freely between these two pores). In a similar fashion, percolation theory can be used with lattice of Figures 1 and 2 to make predictions about the speed of diffusion of electrons from one cell to the other, or indeed whether electrons located in one area of the grid can get to other certain other parts of the grid at all. Furthermore, theories of *Directed Percolation* (Takeuchi *et al.*, 2007) permit such predictions to be made based on the overall topology of the lattice in the presence of a biasing stimulus.

We note the system has no "memory" of what cells were filled or empty in previous generations. This arises because we expect electron movements into or from cells to occur with concomitant change in the volume occupied by that cell: we do not, for example, expect any lag-time between electron movement and cell re-sizing that would allow cells to leave a trail of "visited" cells noticeably different from unvisited empty cells (although if this was observed for some reason this would be interesting). Thus, with no memory effects, the next configuration the filled cells of these CA can take is determined only by the rules governing the system and its current configuration, regardless of the configurations of the system in the past. This means that CA such as those discussed above can be modeled as *Markov Chains* (Markov, 1971). Given a set of rules detailing the likelihood of cellular transformations in a given conformation, it should therefore be possible to work out the probability distribution of the cells in future generations. Hence, elucidation of these guiding rules is critical to a rigorous understanding of the behaviour of such CA. In the next section, we map out how these rules might be determined in real systems and present a practical pathway to a functional device.

The crystal net $\mathbf{1}_{ox}$ (empty cells) can be switched to the reduced version ($\mathbf{1}_{red}$, filled cells) in solution (and back again) by using chemical redox agents (Ritchie, 2008). For practical purposes, switching in the solid state is desirable, without the need for chemical techniques. The ability to switch these Keggin nets *electrically* is thus of primary importance if they are to function as crystalline computational devices. To this end, we propose taking single crystals of the form $[(C_4H_{10}NO)_{40}(W_{72}M_{12}O_{268}Si_7)]\cdot 48H_2O$ ($M = Mn^{III}$ or Co^{II}) and attaching electrodes to their surfaces. Such crystals are approximately tetrahedral and can easily be grown to a size of around 0.5 mm per edge. This makes them amenable to processing using existing well-established and cheap technologies in use throughout the electronics industry. Figure 5 shows a schematic representation of a suggested set-up for electrical signal input, bias and read-out. We propose to use a standard three-electrode configuration for inputting electrical signals into a crystal immersed in a sub-millimeter scale electrolyte-containing cavity. An appropriately sheathed working electrode will be attached to each face of a tetrahedral crystal, whilst the

Figure 5. Stylized 2-D representation of a tetrahedral crystal (red triangle) connected to three different working electrodes (black lines with a lighter shaded area around them symbolizing electrical insulation from the electrolyte medium). An additional contact could be made in the plane orthogonal to the paper.

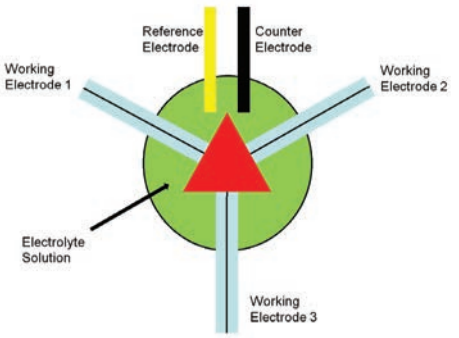

reference and counter electrodes will sit in the electrolyte bath (alternatively, individual reference and counter electrodes could be attached to each face as with the working electrodes). Such structures such are readily accessible using standard microfabrication techniques such as micro-contact printing and allied techniques (Kumar & Whitesides, 1993; Perl *et al.,* 2009).

Input to the crystal lattice can then be achieved by applying a potential between the working and reference electrodes. Two basic types of electrochemical techniques will be tried initially: cyclic voltammetry and bulk electrolysis. In a bulk electrolysis experiment, the potential is held at a constant value as charge is allowed to flow between the working and counter electrodes. Although Keggin nets such as $\mathbf{1}_{ox}$ are not electrically conductive, it is hoped that addition of recyclable redox reagents to the electrolyte bath will stimulate electrically-driven oxidation and reduction reactions within the crystal in the solid state. An assessment of the amount of charge that has to be passed to produce complete transformation of $\mathbf{1}_{ox}$ to $\mathbf{1}_{red}$ will then be undertaken, allowing experiments to be run where only a fraction of this charge is permitted to pass. The effect of passing less than the amount of charge required to convert the entire crystal from one form into another may well produce areas of the crystal where complete reduction has occurred whilst other parts *of the same crystal* remain in the oxidized form. This would correspond to the situation shown in Figures 3 and 4, where islands of reduced (filled cells) appear against a background of empty cells, as is required for CA. These islands will then diffuse through the crystal lattice, in an analogous fashion to the cells of Figures 3 and 4, although now in three dimensions instead of just two. Application of a moderate potential too low to give charge injection into the crystals could then be used to bias the direction of diffusion of these cells, without adding to their number as previously suggested. If different amounts of charge are injected into different faces of the crystal simultaneously, complicated patterns of moving islands of charge could be set up, which would diffuse under the influence of a bias provided by the various working electrodes in a fashion determined by the operator. Hence not only the initial (and subsequent) injections of charge are under direct and/or automated control, but there is also the ability to vary the biasing potentials supplied by the four working electrodes to create highly complex dynamic patterns of cells within the crystal.

An alternative mode of electrical input is *via* cyclic voltammetry. This technique cycles between two voltages specified by the user in a linear fashion, with the rate of scanning between the high and low end voltages also

specified by the user. Normally, an analyte at the electrode surface is (for example) first oxidized (giving rise to a characteristic rise in current as its oxidation potential is reached), and then reduced at the same potential as the potential scan is reversed, giving a characteristic rise in current in the opposite direction to before. At sufficiently low potential scan rates, however, an oxidation (reduction) may occur at one potential but the species which has thus been oxidized (or reduced) has sufficient time to diffuse away from the electrode before the potential sweeps back, and so no corresponding rise in current in the opposite direction is observed: the species cannot be converted back to its original form as it is no longer near enough to the electrode. In a similar way, cyclic voltammetry at sufficiently low scan rates with a solid crystalline sample could set up regular "waves" of filled cells diffusing into the body of the crystal, which could interact and interfere with other such waves from the other electrodes to produce patterns of cells as in Figures 3 and 4. How these waves interact (what rules they follow) is expected to depend strongly on the nature of the crystal through which they are traveling, and so experimenting with signal inputs and sequences will be critical to understanding what computations these CA can perform. Likewise, it will also be crucial to assess what level of control can be achieved concerning initial charge-injection into a given crystal, as CA are highly dependent on their precise starting configurations.

Output from these crystals could also be obtained by *in-situ* electrical detection. Waves propagating through the crystal to an electrode will cause a peak in current to be measured at that electrode (conventional potentiostats can measure currents on the nA scale). By analyzing models of simple inputs and their corresponding outputs and matching these models with the actual outputs from experiment, it is hoped to be able to correlate sequences of signals arriving at the electrodes whilst in their "read" state to computational events occurring within the crystal itself. This should allow a "library" of simple read-outs to be constructed, with which the ideas of Markov and percolation theory can be used to deduce more complex computational outputs *via* interferometry.

COMPUTING WITH SPIN-CROSSOVER COMPLEXES

As noted in the Introduction, certain spin-crossover (SCO) complexes may also be suitable candidates for crystal-based molecular scale computing. Quantum mechanics states that electrons have a property called *spin*, which can take one of only two values: +½ (spin "up") or -½ (spin "down"). An electron on its own in a molecular orbital (an "unpaired" electron) will adopt one of these values at random, although unpaired electrons in neighboring orbitals sit with spins aligned (symbolized by arrows pointing in the same direction in Figure 6a). When two electrons occupy the same orbital (a filled orbital), the electrons are said to *pair* and their spins are necessarily opposite. Thus a filled orbital has zero net spin, whilst the spin of any unpaired electrons can be added together to give an overall net spin for the metal center.

SCO arises in certain transition metal complexes (where the metal center has between 4 and 7 electrons in its outermost *d*-electron shell) that have a low energy barrier between *high spin* and *low spin* forms (Figure 6b). High spin complexes have these *d*-electrons as separate as possible, filling all five *d*-orbitals with individual electrons before any pairing-up of electrons in orbitals occurs. This indicates that the energy penalty for forcing two negatively-charged electrons to occupy the same orbital is greater than the energy gap (Δ) between the t_{2g} and e_g sets of *d*-orbitals (Figure 6b), and so electrons prefer to occupy the higher energy e_g set before they pair-up in the otherwise lower energy t_{2g} set. Having many unpaired electrons in this fashion gives the metal center a high effective *spin* associated with the combined quantum mechanical spins of all the unpaired electrons in these *d*-orbitals. In contrast, low spin complexes have a Δ value larger than the energy for pairing electrons in

Figure 6. (a) An unpaired electron in an orbital (spin = ½, left) and a pair of electrons in the same orbital (spin = 0, right). (b) The high and low spin forms of Fe(II): low spin (left, spin = 0) and high spin (right, spin = 2). Individual electrons are shown as arrows, the direction of which shows whether the spin is "up" (+½) or "down" (-½). Unpaired electrons are arbitrarily assigned as spin up in this example.

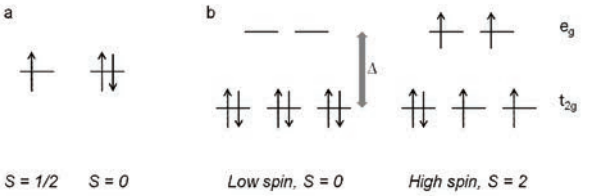

the lower energy t_{2g} set and so all the t_{2g} orbitals fill with paired electrons (with net spin = 0) before any unpaired electrons appear in the e_g set. Figure 6b shows the effect of this on the effective spin of the metal center for the case of the Fe^{2+} ion, which has 6 *d*-electrons and can adopt either high or low spin forms (*vide infra*).

When the factors affecting the relative sizes of Δ and the energy for pairing electrons in orbitals (*i.e.* the factors dictating whether a particular transition metal complex is high or low spin) are delicately balanced, it is sometimes possible to change a metal center from high to low spin (or *vice versa*) by a subtle change in the environment. This is spin cross-over. Large changes in the properties of complexes capable of SCO occur as a result of this transition, especially with regards to magnetic properties.

Analogs of the dye Prussian Blue with formula $A_{2x}Co_{1.5-x}[Fe(CN)_6]\cdot nH_2O$ (A is an alkali metal ion, see Figure 7a) (Dei, 2005, pp. 1160-1163) will serve to illustrate the potential of SCO complexes as CA. At low temperatures (10-20 K) (red) light-induced electron transfer leads to reduction of Co(III) centers (*S = 0*) by Fe(II) centers (*S = 0*) connected to them by CN bridges: Fe^{II}-CN-Co^{III} → Fe^{III}-CN-Co^{II}. The resulting Fe(III) centers then have spins of ½, whilst the Co(II) centers have (*S = 3/2*), giving a material that is highly antiferromagnetically coupled. Back-conversion can then be achieved by irradiation with blue light, restoring the original diamagnetic state. In theory, this change in oxidation state with concomitant change in spin states could be produced optically in defined areas of a solid sample using highly focused laser pulses, or alternatively accessed with molecular-level precision on surfaces by electron-injection from an STM tip. As long as electrons are then free to exchange between metal centers, CA can then be envisioned based on the associated exchange of spins.

A simplified CA lattice based on SCO complexes like these is shown in Figure 7b. Filled cells now represent individual Fe^{III}-CN-Co^{II} centers (high spin state). As with the electrochemically-driven system proposed for polyoxometalate nets of the form $[(C_4H_{10}NO)_{40}(W_{72}M_{12}O_{268}Si_7)]\cdot 48H_2O$, high spin to low spin conversion is often accompanied by a decrease in the volume of the species undergoing this transformation (this is because the e_g set of orbitals has a slight *antibonding character* and is more heavily populated in high spin complexes, hence the metal-ligand bonds in high spin complexes are weaker and longer than in low spin complexes). Thus, we would expect similar arguments about the grouping together of filled and empty cells as was seen with the polyoxometalate nets, and similar rules should apply regarding how different shapes behave. As we now consider an individual Fe^{III}-CN-Co^{II} center to be a cell, the simplest 3-D pattern of cells for a Prussian Blue-based cellular automaton is as face-sharing cubes, which we represent in 2-D as a von Neumann-style grid of squares (Figure 7b).

Figure 7. (a) Idealized schematic of the structure of the Prussian Blue analog $A_{2x}Co_{1.5-x}[Fe(CN)_6]\cdot nH_2O$ at a Co: Fe stiochiometry of 1:1. CN bridges are shown as black lines, Co centers in red and Fe centers in blue. Water molecules and alkali metal ions are not shown for clarity. (b) Stylized 2-D grid for CA based on the structure of Prussian Blue.

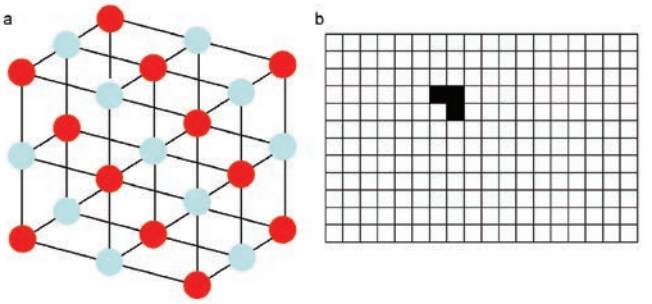

However, as previously noted, such SCO complexes must be kept at very low temperatures if "excited" spin-state configurations produced upon stimulus input (e.g. laser irradiation) are not to immediately decay back to their ground states. Although new discoveries are constantly increasing the threshold temperatures for SCO (Halcrow, 2007), the need for such low temperatures is a major drawback to viable CA computational devices using SCO. Furthermore, the chief input for the type of controlled SCO events necessary for computation is irradiation by laser, which limits the size of devices that can be made as photons cannot be focused accurately within crystal matrices. To realize CA that can work using the whole 3-D lattice of a crystal, alternative inputs to light must be found. An additional technical challenge relates to the phenomenon of SCO cooperativity in the solid state. (Halcrow, 2007). Often the change in size between low and high spin complexes means that SCO tends to happen throughout the entire crystal at the same time, without any intermediate stage such as the formation of islands of filled and empty cells, as is necessary for SCO compounds to act as CA. Engineering SCO compounds that have such an intermediate phase that can be accessed at ambient temperatures and controlled using more penetrating stimuli (such as electrical signals) are therefore the key challenges facing the application of SCO complexes to CA-based computation.

In conclusion we have discussed a radical new computing paradigm based around the idea of implementing a 3D CA within an inorganic framework with nanoscale cellular compartments that can be switched on and off via REDOX processes. We have compared and contrasted this with the spin-cross over materials, and also discussed the possible rules that may define any physical 3D CA. The SC-SC system is particularly important since it represents the first example of a totally new class of reversibly switchable cellular inorganic materials and therefore represents an excellent candidate to explore the first 3D CA. This is exciting since such materials represent a new type of computer 'hardware' (a crystal computer) and the embedded rules the 'software'. As such the main experimental goal is to elucidate the rules experimentally and to do a range of basic computations to that show that the CA is working (and to determine the level of computations of which it is capable), and then to develop algorithms that exploit the massively parallel computing power present in a cellular switchable inorganic crystal.

ACKNOWLEDGMENT

This research was supported in part by grants from the UK EPSRC, the Royal Society / Wolfson Foundation and the University of Glasgow.

REFERENCES

Bandyopadhyay, A., Pati, R., Sahu, S., Peper, F., & Fujita, D. (2010). Massively parallel computing on an organic molecular layer. *Nature Physics*, *6*, 369–375.

Bennett, J. J. (Ed.). (1866). *The miscellaneous botanical works of Robert Brown*. London, UK: Ray Society.

Berlekamp, E. R., Conway, J. H., & Guy, R. K. (2003). *Winning ways for your mathematical plays* (2nd ed.). Wellesley, MA: A K Peters.

Bodenthin, Y., Schwarz, G., Tomkowicz, Z., Lommel, M., Geue, T., & Haase, W. (2009). Spin-crossover phenomena in extended multi-component metallosupramolecular assemblies. *Coordination Chemistry Reviews*, *253*, 2414–2422.

Broadbent, S., & Hammersley, J. (1957). Percolation processes I: Crystals and mazes. *Proceedings of the Cambridge Philosophical Society*, *53*, 629–641.

Credi, A. (2008). Monolayers with an IQ. *Nature Nanotechnology*, *3*, 529–530.

de Silva, A. P., & Uchiyama, S. (2007). Molecular logic and computing. *Nature Nanotechnology*, *2*, 399–410.

Dei, A. (2005). Photomagnetic effects in polycyanometallate compounds: An intriguing future chemically based technology? *Angewandte Chemie International Edition*, *44*, 1160–1163.

Gardner, M. (1970). The fantastic combinations of John Conway's new solitaire game "life". *Scientific American*, *223*, 120–123.

Gütlich, P., Garcia, Y., & Goodwin, H. A. (2000). Spin crossover phenomena in Fe(II) complexes. *Chemical Society Reviews*, *29*, 419–427.

Halcrow, M. A. (2008). Trapping and manipulating excited spin states of transition metal compounds. *Chemical Society Reviews*, *37*, 278–289.

Jones, R. (2009). Computing with molecules. *Nature Nanotechnology*, *4*, 207.

Kumar, A., & Whitesides, G. M. (1993). Features of gold having micrometer to centimeter dimensions can be formed through a combination of stamping with an electrostatic stamp and an alkanethiol "ink" followed by chemical etching. *Applied Physics Letters*, *63*, 2002–2004.

Long, D.-L., Tsunashima, R., & Cronin, L. (2010). Polyoxometalates: Building blocks for functional nanoscale systems. *Angewandte Chemie International Edition*, *49*, 1736–1758.

Markov, A. A. (1971). Extension of the limit theorems of probability theory to a sum of variables connected in a chain. In R. Howard (Ed.), *Dynamic probabilistic systems, volume 1: Markov Chains*. New York, NY: John Wiley & Sons.

Pei, R., Matamoros, E., Liu, M., Stefanovic, D., & Stojanovic, M. N. (2010). Training a molecular automaton to play a game. *Nature Nanotechnology*, *5*, 773–777.

Perl, A., Reinhoudt, D. N., & Huskens, J. (2009). Microcontact printing: Limitations and achievements. *Advanced Materials (Deerfield Beach, Fla.)*, *21*, 2257–2268.

Ritchie, C., Streb, C., Thiel, J., Mitchell, S. G., Miras, H. N., & Long, D.-L. (2008). Reversible redox reactions in an extended polyoxometalate framework solid. *Angewandte Chemie International Edition*, *47*, 6881–6884.

Takeuchi, K. A., Kuroda, M., Chaté, H., & Sano, M. (2007). Directed percolation criticality in turbulent liquid crystals. *Physical Review Letters*, *99*, 234503.

Thiel, J., Ritchie, C., Miras, H. N., Streb, C., Mitchell, S. G., & Boyd, T. (2010). Modular inorganic polyoxometalate frameworks showing emergent properties: Redox alloys. *Angewandte Chemie International Edition*, *49*, 6984–6988.

Thiel, J., Ritchie, C., Streb, C., Long, D.-L., & Cronin, L. (2009). Heteroatom-controlled kinetics of switchable polyoxometalate frameworks. *Journal of the American Chemical Society*, *131*, 4180–4181.

Turing, A. (1937). On computable numbers, with an application to the entscheidungs problem. *Proceedings of the London Mathematical Society*, *42*, 230–265.

Turner, J. W., & Schultz, F. A. (2001). Coupled electron-transfer and spin-exchange reactions. *Coordination Chemistry Reviews*, *219-221*, 81–97.

von Neumann, J. (1951). The general and logical theory of automata . In Jeffress, L. A. (Ed.), *Cerebral mechanisms in behavior – The Hixon symposium* (pp. 1–31). New York, NY: John Wiley & Sons.